Supporting Information for "Electrokinetically-Driven Transport of DNA through Focused Ion Beam Milled Nanofluidic Channels"

Laurent D. Menard and J. Michael Ramsey

Determination of Nanochannel Resistances and Electric Field Strengths

Figure S1 shows a simplified schematic of the chip design, having four access reservoirs for introducing solutions to the chip. The ionic resistance between each reservoir pair was measured using a picoammeter/voltage source (Keithley Model 6487) with a voltage of 5 V applied between reservoirs. These measurements were performed using the buffered electrolyte solutions (2X TBE and 2X TBE with 2 wt% PVP) that were used for transport experiments. The addition of 2 wt% PVP was not found to significantly affect the results. Table S1 presents representative resistances measured in 2X TBE before and after the transport experiments for each of the nanochannel devices. The relative standard deviations in these measurements are <3% and more typically <1%. The resistances of each of the microchannel segments and the nanochannel arrays were calculated from these measured resistances using a least-squares method, assuming simple resistors in series (Table S2). During the transport measurements, a voltage was applied from reservoir 1 to reservoir 3 and the percentages of the applied voltage that was dropped across the nanochannel arrays are given in Table S2. These resistances were stable over repeated experiments performed on the devices over several months. Devices were cleaned and conditioned between experiments by introducing a 10% sulfuric acid solution to the channels, placing the chip in a covered container overnight, and rinsing the channels with distilled deionized water the following morning.

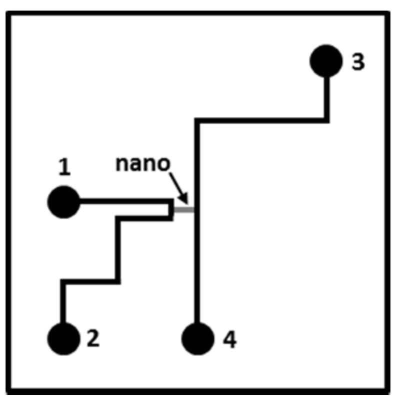

Figure S1. Schematic of the nanofluidic chip design showing the various pathways over which ionic resistances were measured.

Table S1. Resistances (GΩ) measured across various reservoir pairs.

	25-nm channels			50-nm channels			100-nm channels		
Reservoir Pair	Before Transport Experiments	After Transport Experiments	Average	Before Transport Experiments	After Transport Experiments	Average	Before Transport Experiments	After Transport Experiments	Average
1-2	2.33	2.32	2.33	2.11	2.17	2.14	2.08	2.07	2.08
1-3	11.05	11.16	11.11	7.80	7.83	7.82	4.20	4.18	4.19
1-4	10.31	10.27	10.29	7.06	7.11	7.09	3.40	3.41	3.41
2-3	12.18	12.06	12.12	8.29	8.59	8.44	4.93	4.91	4.92
2-4	11.49	11.26	11.38	7.65	7.86	7.76	4.16	4.15	4.16
3-4	2.20	2.22	2.21	2.05	2.05	2.05	2.00	2.01	2.01

Table S2. Individual channel resistances (GΩ).

Channel	25-nm channels	50 nm-channels	100-nm channels
microchannel 1	0.64	0.74	0.67
microchannel 2	1.69	1.40	1.41
microchannel 3	1.50	1.38	1.39
microchannel 4	0.70	0.67	0.62
nanochannel array	8.97	5.68	2.13
% voltage dropped across array	**81%**	**73%**	**51%**

We note that the measured resistances for the nanochannels are consistently less than those predicted from a simple calculation based on the nanochannel dimensions:

$$R_{nano} = \rho L_{nano}/A_{nano} \tag{S1}$$

where R_{nano} is the ionic resistance through the nanochannel, ρ is the solution resistivity (556 Ω cm for 2X TBE), L_{nano} is the nanochannel length, and A_{nano} is the nanochannel cross-sectional area. The devices used in these studies consisted of arrays of ten nanochannels with identical dimensions, such that the array resistance was ten-fold lower than that of a single nanochannel. The calculated resistances do not account for surface conductance contributions that are expected to be significant in nanochannels or for leakage currents associated with bonding defects or scratches in the substrate surface. The FIB milled nanochannels are spaced sufficiently to prevent networks of these leakage pathways that could complicate electric field determinations, as evidenced by images of fluorescent dye solutions in the nanochannels and by the constant velocity of DNA transport. These observations reinforce the importance of using the resistances measured in each of the electrolyte solutions used in the transport experiments rather than theoretical values and avoiding extrapolation across a range of ionic strengths.

As a final note, we consider the access resistance to the nanochannels. While the access resistance can be quite significant in the case of nanopores fabricated or assembled in thin membranes,[1,2] it is negligible for sufficiently long nanochannels such as the 50-μm long channels used in this study. The total access resistance (R_{access}) for the two ends of a cylindrical nanochannel is:

$$R_{access} = \rho/d_{nano} \tag{S2}$$

where d_{nano} is the nanochannel diameter.[3] In 2X TBE, the access resistances for the 25-nm, 50-nm, and 100-nm channels are approximately 0.22 GΩ, 0.11 GΩ, and 0.06 GΩ, respectively, or <0.3% of the resistance of a single nanochannel.

Roughness of the Bottom Surface of a Focused Ion Beam Milled Nanochannel

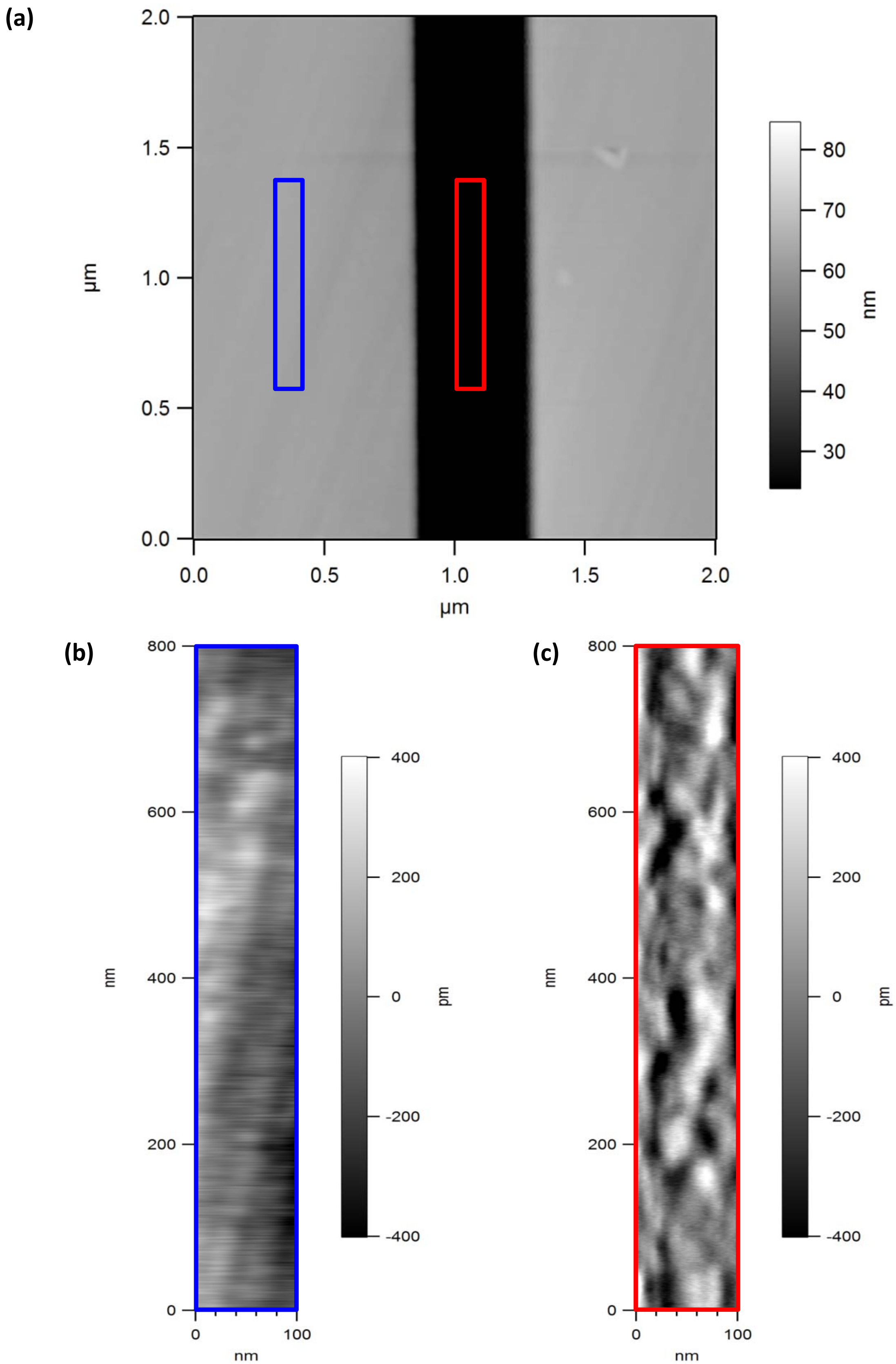

Figure S2. Atomic force microscopy (AFM) characterization of a 400-nm wide x 400-nm deep nanochannel fabricated by FIB milling in a quartz substrate. A channel of this size was chosen to ensure that the bottom surface of the nanochannel could be profiled without interference due to tip-wall interactions. Scans were performed in tapping mode on an Asylum Research MFP-3D atomic force microscope using a silicon tip with a tip radius ~2 nm (Applied Nanostructures). (a) Scan of the nanochannel and the adjacent quartz surface. (b) High resolution scan of the quartz surface adjacent to the nanochannel; rms roughness is 144 pm (c) High resolution scan of the bottom of the nanochannel; rms roughness is 196 pm.

REFERENCES

(1) Garaj, S.; Hubbard, W.; Reina, A.; Kong, J.; Branton, D.; Golovchenko, J. A. *Nature* **2010**, *467*, 190-193.

(2) Wanunu, M.; Dadosh, T.; Ray, V.; Jin, J.; McReynolds, L.; Drndić, M. *Nat. Nanotechnol.* **2010**, *5*, 807-814.

(3) Hall, J. E. *J. Gen. Physiol.* **1975**, *66*, 531-532.